Efficient adsorption of Cu(II) and Cr(VI) metal ions by Schiff base modified SBA-15

Farshad Boorboor Ajdari, Mahdi Behzad*

Department of Chemistry, Semnan University, Semnan 35351-19111, Iran

Abstract

SBA-15 was functionalized with amine ($-NH_2$) and 3-methoxy salicylaldehyde (3-MS) to form a mesoporous silica with Schiff base modified surface (3-MS–SBA-15). The materials were characterized and analyzed by Fourier transform infrared (FT-IR), scanning electron microscopy (SEM), Nitrogen adsorption-desorption (BET), and X-ray diffraction (XRD) spectroscopy. The removal of Cu(II) and Cr(VI) metal ions onto 3-MS-SBA-15 was then studied from their aqueous solutions in order to investigate and optimize the effect of contact time, solution pH, adsorbent dose and temperature in batch system. The equilibrium data were analyzed using the Tempkin, Dubinin- Radashkovich, Langmuir and Freundlich isotherms. Freundlich and Langmuir isotherms were well fitted for Cu(II) and Cr(VI) adsorption process, respectively. The kinetics analyses showed that the total adsorption process was completely fitted with the pseudo-second-order kinetics model. The adsorption depended strongly on temperature, as the adsorption capacity decreased for Cu(II) while increased for Cr(VI) by increasing the temperature of the system, indicating the exothermic and spontaneous nature for Cu(II) and the endothermic and spontaneous nature for Cr(VI).

Keywords: adsorption, removal, Cu(II), Cr(VI), kinetics, thermodynamics

1. Introduction

Water is one the most important resources for living. Water purification and water treatment can help return waste water into water cycle. Heavy metal ions such as Cr(VI), Cu(II), Pb(II), Co(II) and etc are among the most important pollutants of water resources which endanger human life. Therefore, various methods have been developed for removing heavy metal ions from wastewater including flotation and electrochemical processes, chemical precipitation, ion-exchange, adsorption, membrane filtration [1, 2].

Adsorption is a reliable, fast and promising technique to remove aqueous pollutions. Adsorption of heavy metal ions by functionalized mesoporous materials has been extensively studied in the past decade. SBA-15 is one the best known silica mesophases. It has been studied in various fields such as catalysis and water treatment due to its narrow pore size distribution, large surface area ($600–1000 \ m^2 \ g^{-1}$) and large and tunable pore diameter (5–30 nm). In addition, a large number of functionalities have been anchored to SBA-15 to modify and improve its efficiency and selectivity and to develop novel materials for a variety of applications.

* **Corresponding author email:** mbehzad@semnan.ac.ir, mahdibehzad@gmail.com. Tel: +98-231-3366195

Examples include –NH$_2$-SBA-15 [3], –SH -SBA-15 [4], –COOH-SBA-15 [5], SA-SBA-15[6] and pyridine-SBA-15 [7]. In the field of water purification, several surface modified SBA-15 have been studied. Many factors which can affect adsorption process such as pH, temperature, adsorbent dosage and contacting time have also been studied [8–10]. In this study, 2-Hydroxy-3-methoxybenzaldehyde was added to NH$_2$-SBA-15 in order to synthesize 3-methoxybenziliden-SBA-15 (3-MS-SBA-15) (figure 1) to remove Cr(VI) and Cu(II) from aqueous solutions. 2-Hydroxy-3-methoxybenzaldehyde was deliberately chosen since it could provide more coordination spheres and hence could provide better adsorption and removal of the ions. Different parameters like temperature, adsorbent dosage and contacting time were optimized.

2. Experimental

2.1. Chemicals and reagents

Pluronic P123 non-ionic surfactant was purchased by Sigma Aldrich. Tetra ethyl ortho silicate (TEOS 98%), 3-aminopropyltrimethoxysilane (APTES 99%), hydrochloric acid (HCl, 37%), ethanol, toluene, Cu (NO$_3$)$_2$ and K$_2$Cr$_2$O$_7$ were obtained from Merck chemicals company. All the studies were performed in aerobic conditions unless otherwise noted. The solvents were of analytical grade and were used without further purifications.

2.2. Characterization of adsorbents

Powder X-ray diffraction (XRD) patterns of materials were recorded from 10.0 to 90.0$^{°}$ by XRD diffractometer (D8 Advance, Bruker) using Cu Kα radiation. The morphology of the materials was obtained by electron scanning microscopy (SEM) (AIS2100, Seron Technology). Nitrogen adsorption–desorption isotherms were obtained at 77.3 K using a volumetric adsorption analyzer in order to determine the textural properties. Approximately 0.37 g of all samples was degassed at 100 °C for 30 min under argon gas flow before analysis. The specific surface area was measured using the Brunauer–Emmett–Teller (BET) method, and the pore size distribution was calculated by applying the Barrett–Joyner–Halenda (BJH) method. Pore volume of materials was also measured. Fourier transform infrared spectra (FT-IR) were recorded (Shimadzu FT-IR 8400S spectrometer, Japan) in the range of 400-4000 cm^{-1} in order to characterize functional groups. The concentration of the metal ions in the solutions was measured using atomic absorption spectrophotometer (Shimadzu AA680, Japan).

2.3. Synthesis of mesoporous silica materials

2.3.1. Synthesis of SBA-15 mesoporous silica

Mesoporous silica SBA-15 was synthesized by the hydrothermal method using TEOS as silica source, Pluronic P123 as template, and HCl to make the media acidic. Briefly, 4 g P123 block copolymer was dissolved in 90 mL 2M HCl and 2l mL distilled water. This solution was stirred for 5 h at room temperature. Then, 6.4 g TEOS was slowly added to that solution and stirred for 24 h at 80 °C. After that the mixture was aged at 100 °C for 24 h in vacuum oven. The mixture was then allowed to cool down to room temperature. The white solid product was filtered, washed with same volume of distilled water and ethanol in order to remove partial surfactant and dried. The solid was calcined at 600 °C for 6 h in furnace to completely remove the surfactant template and finally the white powder of SBA-15 was obtained [13-14].

2.3.2. Synthesis of NH$_2$–SBA-15 mesoporous silica

The amine functionalized SBA-15 was prepared according to the method described in the literature [12]. Briefly, 5 g of calcined SBA-15 was dried in a vacuum oven for 12 h at 100 °C to be activated and then suspended in 250 mL dried toluene. Then 7 mL APTES was added to the mixture and refluxed for 24 h (Figure 1). Finally, NH$_2$–SBA-15 was filtered and washed with dried toluene and collected [12].

2.3.3. Synthesis of 3-MS–SBA-15 mesoporous silica

At first 2 g of NH$_2$–SBA-15 was dried in vacuum oven at 100 °C for 2 h to be activated, then dissolved in 150 mL dried toluene. 2 g of 3-methoxy salicyl aldehyde was then added to that solution and refluxed at 150 °C for 24 h. At the end, yellow solid was collected by filtration and washed with dried Toluene (Figure 1).
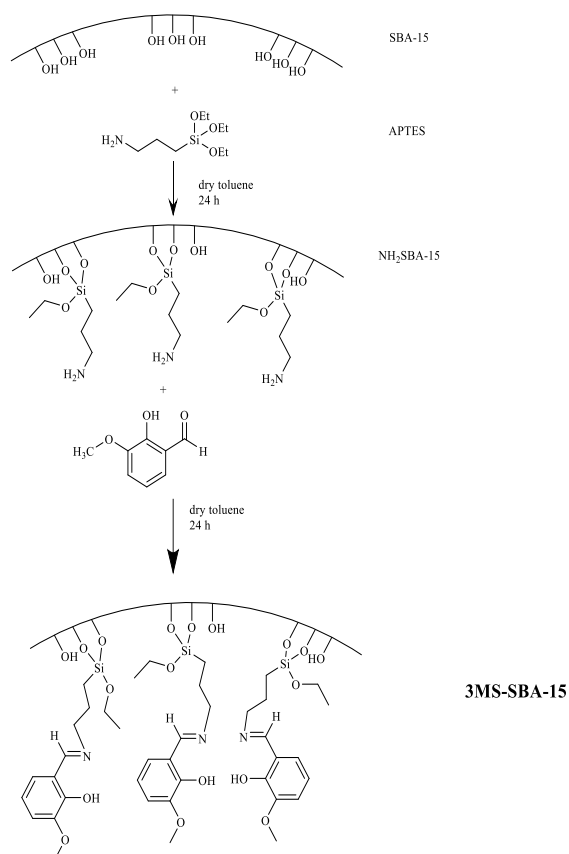

Figure 1. Schematic representation of the synthesis of NH$_2$-SBA-15 and 3-MS-SBA-15

2.4. Batch adsorption experiments

Batch adsorption experiments were performed in 50 mL bakers containing 10 mL Cu (NO$_3$)$_2$ and K$_2$Cr$_2$O$_7$ (50 mg.L^{-1}) solutions being stirred at 150 rpm at room temperature. The solutions of Cu (II) and Cr (VI) ions were prepared by dissolving an exact amount of Cu (NO$_3$)$_2$ and K$_2$Cr$_2$O$_7$ in de-ionized water to prepare standard and sample solutions.

2.5. Removal efficiency

The removal efficiency of the metal ions was calculated by the following equation (1):

$$R = ((C_0 - C_t)/ C_0) \times 100 \qquad \text{eqn. (1)}$$

Where R is the removal efficiency of the metal ions, C_0 (mg.L^{-1}) the initial concentration and C_t (mg.L^{-1}) the concentration of the metal ions at time t.

2.6. Adsorption capacity

Adsorption capacity of the adsorbent was calculated by equation (2):

$$q_e = ((C_0 - C_e)V)/ W \qquad \text{eqn. (2)}$$

where qe (mg.g^{-1}) is the equilibrium adsorption capacity of the adsorbent, C_0 (mg.L^{-1}) is the initial concentration and C_e (mg.L^{-1}) is the concentration at equilibrium of metal ions, V(L) is the volume of metal ions solution and W(g) is the weight of the adsorbent.

2.7. Effect of the solution pH

The effect of the different solution pH values on the adsorption process was studied by mixing 0.02 g of 3-MS–SBA-15 in 10 mL of a solution containing 50 mg L^{-1}of Cu (II) and Cr (VI) metal ions. The pH range from 2 to 6 was set using 1M HCl and 0.1M NaOH solution. The baker content was agitated at 150 rpm using stirrer (D110, Alpha, China) to reach equilibrium. The concentration of the remaining metal ions in aqueous phase was measured. The pH = 5 was chosen as the optimized value to remove both Cu (II) and Cr (VI) metal ions.

2.8. Effect of the adsorbent dose

The effect of the dose of 3-MS–SBA-15 on the adsorption of 50 mg.L^{-1} solution of Cu(II) and Cr(VI) metal ions were investigated using 0.005 0.01, 0.02, 0.03, 0.04, 0.05 g adsorbents. By adding a fresh dilution of 0.1M NaOH, the pH of the solution was adjusted to 5. Finally the best dose for removing of metal ions was obtained at 0.05 and 0.04 for Cu (II) and Cr(VI) metal ions, respectively.

2.9. Effect of the contact time

In order to investigate the effect of mixing time optimized amount of the adsorbent was added to Cu (II) and Cr (VI) solutions. The mixture was stirred in the range of 5 to 120 min at room temperature. The mixture was then filtered, and the concentration of the remaining metal ions was measured. 120 min and 60 min were obtained as the optimized time for the removal of Cu (II) and Cr (VI) metal ions, respectively.

2.10. Effect of temperature

The effect of temperature was investigated at different temperatures ranging from 273 to 308 K for both metal ion solutions. Adsorption was conducted under optimized conditions obtained in previous sections.

2.10. Adsorption isotherms

The adsorption isotherms were considered at equilibrium conditions in order to study the relationship between the amount of adsorbed metal ions and the concentration of remaining metal ions in the aqueous phase. These adsorption data were fitted to different models including Langmuir, Freundlich. The Langmuir isotherm describes the monolayer sorption onto the surface of the sorbent.

Langmuir isotherm is represented by equation 3 [15]:

$$q_e = (q_m b C_e)/ (1 + bC_e) \qquad \text{eqn. (3)}$$

Where q_e (mg.g^{-1}) is the equilibrium adsorption capacity of the sorbent and C_e (mg.g^{-1}) is the concentration of metal ions at equilibrium. The q_m(mg.g^{-1}) is the maximum capacity of the metal ion which could be adsorbed, and b (L.mg^{-1}) is the constant of the adsorption bonding energy. The Freundlich isotherm model describes multilayer sorption and sorption on heterogeneous surfaces. The Freundlich isotherm is represented by the following equation (eqn. (4)) [16]:

$$q_e = K_f \, C_e \, /(1/n) \qquad \text{eqn. (4)}$$

Where q_e (mg.g^{-1}) is the equilibrium adsorption capacity of the adsorbent, C_e (mg.L^{-1}) the concentration of metal ions at equilibrium, KF is empirical constant adsorption value of Freundlich isotherm, and n is the empirical constant which depends on the heterogeneity of the adsorbent that indicates the intensity of adsorption.

2.11. Adsorption kinetics

The adsorption kinetics studies were investigated using 0.05 and 0.04 g of 3-MS–SBA-15 in 10 mL of 50 mg.L^{-1} solutions of Cu(II) and Cr(VI) metal ions under previously obtained optimized conditions. The pseudo-first-order and the pseudo-second-order models were investigated using equations 5 and 6, respectively.

$$\text{Log } (q_e - q_t) = \text{Log } q_e - (k_1/2.303)t \qquad \text{eqn. (5)}$$

$$(t / q_t) = 1/(K_2 q_e^2) + t/ q_e \qquad \text{eqn. (6)}$$

Where q_e(mg g^{-1}) is the adsorbed metal on the adsorbent at equilibrium and q_t (mg g^{-1}) is the adsorbed metal on the adsorbent at time t, k_1 is the rate constant of first-order adsorption in min^{-1} and k_2 is the rate constant of second-order adsorption in g mg^{-1} min^{-1}. In this study pseudo-second-order model was well fitted for both Cu (II) and Cr (VI) metal ions.

2.12. Adsorption thermodynamics

The adsorption studies were carried out at different temperatures including 273, 278, 283, 288, 293, 298 and 308 K to investigate thermodynamic criteria. Using the initial and the equilibrium concentrations (C_0 and C_e) of the metal ions the distribution coefficient (k_d) was evaluated by following equation 6:

$$k_d = ((C_0 - C_e)/ C_e) \times (V/W) \qquad \text{eqn. (6)}$$

Where V (mL) is the working volume and W (g) is the adsorbent mass.

And then the enthalpies (ΔH^0) and entropies (ΔS^0) were calculated from equation 7.

$$\text{Ln } k_d = \Delta S^0/ R - \Delta H^0/RT \qquad \text{eqn. (7)}$$

By drawing ln k_d versus 1/T plots the ΔH^o (J mol^{-1}) and ΔS^o (J mol^{-1} K^{-1}) were obtained from the slope and intercept of patterns, respectively. T (K) is the temperature and R is the universal gas constant (8.314

J mol^{-1} K^{-1}). The Gibbs free energy (J mol^{-1}), expressed by ΔG^0, was calculated according to the equation 8:

$$\Delta G^0 = \Delta H^0 - T \, \Delta S^0 \qquad \text{eqn. (8)}$$

3. Results and discussions

3.1. Characterization of the adsorbent

The XRD spectra for SBA-15, 3-MS–SBA-15, and after adsorption Cu-3-MS-SBA-15 and Cr-3-MS – SBA-15 are shown in figure 2a, 2b, 2c and 2d, respectively. All materials exhibited a single strong peak in their XRD pattern. Consequently, the anchoring of 3-methoxy salicylaldehyde inside the mesoporous channels of SBA-15 did not seriously perturb the overall ordered structure of the mesoporous silica [16]. The intensities of the XRD peaks for 3-MS–SBA-15, Cu-3-MS-SBA-15 and Cr-3-MS –SBA-15 are approximately the same while according to Debye-Scherrer equation size of 3-MS–SBA-15, Cu-3-MS-SBA-15 and Cr-3-MS –SBA-15 was calculated 18.43, 16.17 and 18.42 nm that shows a substantial decrease in size of Cu-3-MS-SBA-15 and also based on Bragg's law the space of plates obtained 0.1548 , 0.1523, 0.1543 Å respectively, that indicates 3-MS–SBA-15 has experienced a constriction after Cu(II) and Cr(VI) metal ions trapping as this constriction for Cr(VI) is more than Cu(II) metal ion. The morphology of the 3-MS–SBA-15 was analyzed by a scanning electron microscope. A typical image is represented in figure 3, which shows many rope-like domains with relatively uniform size. The results for N$_2$ adsorption–desorption containing the pore diameters (DBJH), the BET surface area (SBET) and the total pore volumes (V$_{total}$) of the calcined 3-MS–SBA-15 and SBA-15 samples are summarized in Table 1. In comparison with SBA-15, average particle size has increased by 28.6 nm while Surface Area and pore volumes have decreased by 209.738 m^2 g^{-1} and 0.391 nm, respectively. FT-IR identified the incorporation of amine groups and 3-methoxy salicylidene functional groups into the SBA-

15 pores. The typical Si–O–Si bands at 432, 810 cm^{-1} are present in all samples and are attributed to the condensed silica network [17]. SBA-15 was reported to exhibit a strong absorption band at about 3448 cm^{-1} (SBA-15 spectrum), attributed to the –OH stretching vibrations of Silanol groups [18]. The band at about 3448 cm^{-1} that is overlapped by the band of NH$_2$ functions, decreased the intensity of peak for the NH$_2$– SBA-15 sample (NH$_2$–SBA-15 spectrum), indicating the presence of primary amine [17]. The new bands at 1662 cm^{-1} (3-MS–SBA-15 spectrum) are indicative of –C=N band in the 3-MS–SBA-15 sample and confirm that the 3-methoxy salicyl aldehyde-based adsorbent is formed [19, 20]. These results confirm the successful functionalization of SBA-15 with amino propyl and 3-methoxy salicyl aldehyde groups.
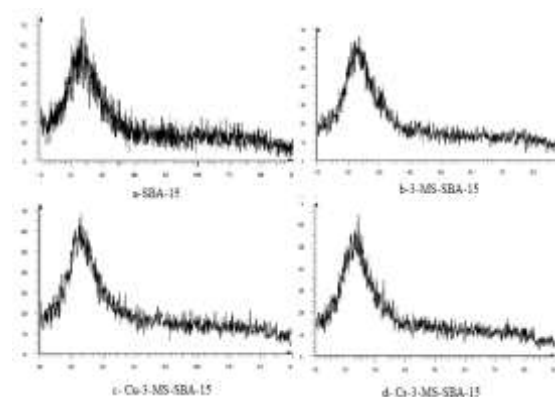

Figure 2. XRD pattern for a-SBA-15, b-3-MS-SBA-15, c-Cu-3-MS-SBA-15, d- Cr-3-MS –SBA-15

Table1. BET properties of SBA-15 and 3-MS-SBA-15

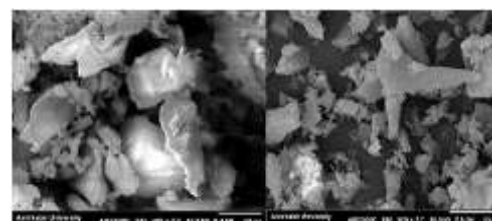| Compound	Average Particle Size (nm)	BET Surface Area (m^2 g^{-1})	average pore width (nm)	Pore volume cm^3 g^{-1}
SBA-15	8.77 nm	689.03	7.3	1.2
3-MS-SBA-15	28.6	209.74	7.4	0.391

Figure 3. SEM micrographs of 3-MS-SBA-15

3.2. Adsorption of Cu (II) and Cr (IV) metal ions in batch system

3.2.1. Effect of pH

The ionic forms of the functional groups on the surface of SBA-15, metal speciation in solution and the competition between proton ions and metal ions are some factors to investigate the effects of the solution pH [21, 22]. Therefore, the pH was optimized in this study while temperature, dose of 3-MS-SBA-15 (adsorbent), and concentration of metal ions were kept constant. The Cu (II) metal ion uptake increased while increasing the pH from 2 to its maximum at pH = 5, and decreased at the pH values higher than 5 because of precipitation. For Cr (VI) metal ions removal, on the other hand, removal decreased by increasing pH values thus pH = 2 was introduced as the maximum removal efficiency point for this ion. The removal efficiency was 52.7 % and 87.9 % for Cu (II) and Cr (VI), respectively, at max pH value. To analyze this results, at low pH values there is an excessive protonation of the adsorbent active sites, resulting in a decrease in the sorption of Cu (II) metal ions whereas Cr (VI) ions changed to $Cr_2O_7^{2-}$ and an electrostatic force between oxyanions and cations increased the removal efficiency [21,22]. At high pH values, the solubility of metal ions was also reduced because of precipitation of solid metal hydroxides.

3.2.2. Effect of adsorbent dose

The experiments were performed to find appropriate adsorbent dose for Cu (II) and Cr (VI) metal ions removal. 3-MS–SBA-15 shows much large heavy metal ions removal efficiency, which might be due to the grafted 3-methoxy salicyl aldehyde groups on the surface of silica and its more active adsorption sites and annular shapes. Physico-chemical properties of metal ions such as electro-negativity and ionic radius may be responsible for the selectivity of Cr (VI) > Cu (II). The higher removal efficiency of 3-MS-SBA-15 indicates a higher loading capacity of metal ions and also revealed that the metal removal percentage

depends strongly on the optimal increase of the adsorbent dose, due to a consequential increase in interference between binding sites at the higher dose. The maximum metal ions removal was obtained 5 and 4 g L^{-1} 3-MS-SBA-15 for Cu (II) and Cr (VI) and was almost the same even at higher doses.

3.2.3. Adsorption isotherms

In order to study the adsorption capacities for metal ions, the surface properties and affinity of the adsorbent, constant values of adsorption isotherms are studied. The b, q_m, n, K_f values and the nonlinear regression correlation coefficients (R^2) for Langmuir and Freundlich isotherms are collected in Table 2. Both isotherms showed a sharp initial slope indicating that the adsorbent operates at high efficiency at a low metal ion concentration and gets saturated with an increased ions concentration. The correlation coefficients indicate that adsorption was fitted better by the Langmuir $R^2 = 0.97$, 0.99 and the Freundlich model $R^2 = 0.98$, 0.97 for Cu (II) and Cr (VI) ions, respectively. Therefore, the adsorption process can be described by the formation of monolayer coverage of the adsorbate on the adsorbent surface. K_f, the Freundlich constant representing the adsorption capacity of the adsorbent, was determined as 0.07 and 13.87 for Cu (II) and Cr (VI), respectively. These values showed a trend similar to that of the Langmuir constant, q_m. The value of n represents the measure of both the relative magnitude and diversity of energies associated with Cu (II) and Cr (VI) adsorption onto 3-MS–SBA-15 and the numerical values of 1/n for all metal ions that lie at < unity, indicating that the marginal adsorption energy decreases with increasing surface concentration and that the Cu (II) and Cr (VI) ions are favorably adsorbed by 3MS–SBA-15 [23]. According to calculations found that Freundlich and Langmuir are fitted to Cu (II) and Cr (VI) respectively.

Table 2. Langmuir and Freundlich isotherms data for a) Cu (II) and b) Cr (VI),

a) Isotherm data for Cu(II)

Langmuir	q_m	K_L	R^2
	0.2734	0.1785	0.9725
Freundlich	K_F	n	R^2
	0.07326	2/91	0.9893

b) Isotherm data for Cr (VI)

Langmuir	q_{max}	K_L	R^2
	0.046	0.17651	0.9982
Freundlich	K_F	n	R^2
	0.1387	2/25	0.9737

Table 3. Kinetics data for a) Cu (II) and b) Cr (VI) in pseudo-first-order and pseudo-second-order models.

a) kinetic data for Cu(II)

pseudo-first-order	Q_1	K_L	R^2
	13.38	212820	0.7308
pseudo-second-order	Q_2	K_2	R^2
	14.28	0.009	0.9994

b) kinetic data for Cr(VI)

pseudo-first-order	Q_1	K_L	R^2
	22.53	0.0305	0.9537
pseudo-second-order	Q_2	K_2	R^2
	22.57	4.140	1

3.2.4. Adsorption kinetics

The rate of metal ions adsorption was studied by fitting the experimental data to pseudo-first order and pseudo-second-order kinetics models that defines the efficiency of sorption for both Cu (II) and Cr (VI). As shown in table 3, parameters of the kinetic models and the regression correlation coefficients (R^2) were calculated which indicate the validity of the pseudo-first-order and pseudo second- order kinetics. In this study, the removal efficiency increased sharply during 115 min and 60 min for Cu (II) and Cr (VI), respectively. The matrix of the adsorbent and the metal ionic radius are two important factors related to adsorption rate [24]. Based on Table 3, Cu (II) ions with a smaller ionic radius showed the higher adsorption rate that can be related to this fact that the Cr (VI) ions can wins in the ions competition for occupying the active sites. By calculating R^2 it was found that the pseudo-second order kinetics model better fitted the kinetics data of the adsorbent 3-MS–SBA-15. As shown in Table 3, the pseudo-second order constants increased from 9.05 to 13.37 min^{-1} for Cu (II) and from 0.22 to 2.66 min^{-1} for Cr (VI). According to table 3 it was found that higher adsorption depends on large pore diameter and volume and higher adsorption rate depends on pore connectivity.

3.2.5. Adsorption thermodynamics

The linear plot of ln k_d versus 1/T was drawn in order to study the effect of temperature on the adsorption of Cu (II) and Cr (VI) metal ions onto 3-MS–SBA-15 and also correlation coefficients and other parameters were calculated and listed in Table 4. The negative value of ΔH^o for Cu (II) and positive value of ΔH^o for Cr (VI) metal ions indicate that this process is exothermic for Cu(II) and endothermic for Cr (VI) metal ions onto the 3-MS–SBA-15. Existence of a high number of adsorption sites on the surface of SBA-15 is the reason of nature of adsorption as those improve metal ions adsorption [23]. In addition, the Gibbs free energy and Entropy were calculated for both Cu (II) and Cr (VI) metal ions and are reported in table 4. By increasing temperature, ΔG^o for Cu (II) decreased from 6.404 to -0.409 kJ mol^{-1} and also ΔS^o increased from - 0.11 to - 0.084 kJ mol^{-1} K^{-1}. ΔG^o and ΔS^o were also calculated for Cr (VI) metal ion. By increasing temperature ΔG^o decreased from – 5.38 to – 11.29 kJ mol^{-1} and ΔS^o decreased from 0.1504 to 0.1386 kJ mol^{-1} K^{-1}, indicating that this sorption has a spontaneous nature. Table 5 indicates a camparision between 3-MS-SBA-15 and other adsorbents

24.377 kJ mol^{-1} - $\Delta H^0_{Cu}= \Delta H^0_{Cr}= 31.480$ kJ mol^{-1}

Table 4. Thermodynamic data for a) Cu (II) and b) Cr (VI)

Table 5. optimum parameters for SBA/EnSA, NZVIs/SBA-15, TS-SBA-15 and 3-MS-SBA-15 for Cr removal

Parameters Adsorbent	pH	Adsorbrnt dose (g/L)	Contact time (min)	Ref.
SBA/EnSA	4	20	15	[27]
NZVIs/SBA-15	5.5	20	10	[28]
TS-SBA-15	6.5	0.5	360	[29]
3-MS-SBA-15	5	4	60	-

was found as an efficient adsorbent for heavy metal ions in aqueous solutions for both Cu (II) and Cr (VI)

Thermodynamic data for Cu(II)				
Temp.(K)	278	283	288	293	298
ΔG^0 (kj/mol)	6.404	4.034	2.321	1.016	-0.409
ΔS^0 (kj/molK)	-0.1102	-0.1003	-0.927	-0.0866	-0.0804

Thermodynamic data for Cr(VI)			
Temp.(K)	273	288	298	308
ΔG^0 (kj/mol)	5.381	-11.863	-11.489	-11.209
ΔS^0 (kj/molK)	0.135	0.1504	0.1441	1386

in batch system.

4. Conclusion

This investigation claims that the 3-methoxy salicylaldehyde grafted to SBA-15 mesoporous silica (3-MS–SBA-15) was prepared and used as adsorbent for the removal of Cu (II) and Cr (VI) ions from aqueous solution in batch system and showed high efficiency. The optimum pH value for removal was 5 and 2 for Cu (II) and Cr (VI), respectively. The Langmuir isotherm fitted the equilibrium data for Cr (VI) and the Freundlich isotherm fitted for Cu(II), with a higher correlation coefficient. The kinetic adsorption onto 3-MS–SBA-15 revealed both ions were adsorbed satisfactorily according to the pseudo-second-order equation. The thermodynamic parameters such as changes in Gibbs free energy (ΔGº), entropy (ΔSº) and enthalpy (ΔHº) were calculated at different temperatures. The value of the Gibbs free energy of adsorption decreased for both heavy metal ions that showed the process was spontaneous, and entropy increased for Cu (II) and reduced for Cr (VI). In addition enthalpy obtained in negative value for Cu (II) and positive value for Cr (VI) which showed the adsorption was exothermic for Cu (II) and endothermic for Cr (VI). To sum up 3-MS-SBA-15

References

[1] G. Ghasemzadeh, M. Momenpour, F. Omidi, M. R. Hosseini, M. Ahani, A. Barzegari, *Front. Environ. Sci. Eng.*, 8, 471-482 (2014).

[2] Z. Chen, S. Deng, H. Wei, B. Wang, J. Huang, G. Yu, *Front. Environ. Sci. Eng.* 7, 326 (2013).

[3] L. Zhang, C. Yu, W. Zhao, Z. Hua, H. Chen, L. Li, J. Shi, *J Non-Cryst. Solids.* 353, 4055 (2007).

[4] A. M. Liu, K. Hidajat, S. Kawi, D. Y. Zhao, *J Chem. Commun.* 13, 1145 (2000).

[5] M. C. Bruzzoniti, A. Prelle, C. Sarzanini, B. Onida, S. Fiorilli, E. Garrone, *J. Sep. Sci.* 30, 2414 (2007).

[6] L. Zhang, X. Hu, C. Yu, R. Crawford, A. Yu, , Int *J. Environ. Anal. Chem*. 93, 1275 (2013).

[7] H. Ebrahimzadeh, A. A. Asgharinezhad, N. Tavassoli, O. Sadeghi, M. M. Amini, F. Kamarei, *Intern. J. Environ. Anal. Chem*, 92, 509 (2012).

[8] E. Da'na, A. Sayari, *Chem. Eng. J.* 166, 445 (2011).

[9] E. Da'na, N. D. Silva, A. Sayari, *Chem. Eng. J.* 166, 454 (2011).

[10] E. Da'na, A. Sayari, *Chem. Eng. J*. 167, 91 (2011).

[11] J. Li, T. Qi, L. Wang, C. Liu, Y. Zhang, *Mater. Let*. 61, 3197 (2007).

[12] H. Lee, J. Yi, Separ. Sci. Technol., 36, 2433 (2001).

[13] L. Hajiaghababaei, B. Ghasemi, A. Badiei, H. Goldooz, M. R. Ganjali, G. Mohammadi Ziarani, J. ENVIRON. SCI., 24, 1347 (2012).

[14] M. W. McKittrick, C. W. Jones, *Chem. Mater*. 15, 1132 (2003).

[15] D. Zhao, J. Feng, Q. Huo, N. Melosh, G. H. Fredrickson, B. F. Chmelka, G. D. Stucky, *Science*. 279, 548 (1998).

[16] M. S. Morey, S. O'Brien, S. G. D. Schwarz, *Chem. Mater.* 12, 898 (2000).

[17] Y. Ho, J. Porter, G. McKay, *Water, Air, Soil Pollut*. 141, 1 (2002),

[18] M. Kruk, M. Jaroniec, C. H. Ko, R. Ryoo, *Chem. Mater*. 12, 1961 (2000).

[19] G. Socrates, *John Wiley & Sons*, Ltd (2004).

[20] Y. Jiang, Q. Gao, H. Yu, Y. Chen, F. Deng, Micropor. Mesopor. Mat., 103, 316 (2007).

[21] Z. Liang, B. Fadhel, C. J. Schneider, A. L. Chaffee, Micropor. Mesopor. Mat., 111, 536 (2008).

[22] S. Yoo, J. D. Lunn, S. Gonzalez, J. A. Ristich, E. E. Simanek, D. F. Shantz, *J. Chem. Mater*. 18, 2935 (2006).

[23] A. Benhamou, M. Baudu, Z. Derriche, J. P Basly, *J. Hazard. Mater.* 171, 1001 (2009).

[24] A. Heidari, H. Younesi, Z. Mehraban, *J. Chem. Eng. J.* 153, 70 (2009).

[25] A. Shahbazi, H. Younesi, A. Badiei, CHEM ENG J. 168, 505 (2011).

[26] X. Jing, F. Liu, X. Yang, P. Ling, L. Li, C. Long, A. Li, *J. Hazard. Mater*. 167, 589 (2009).

[27] L. Dolatyari, M. R. Yaftian, S. Rostamnia, J. Environmental Management 8, 169 (2016).

[28] X. Sun, Y. Yan, J. Li, W. Han, L. Wang, J. Hazardous Materials, 26, 266 (2014).

[29] S. Parambadath, A. Mathew, M. J. Barnabas, S. Y. Kim, C. S. Ha, J Sol-Gel Sci Technol, (2015)   (doi:10.1007/s10971-015-3923-x)